ELSEVIER

Earth and Planetary Science Letters 195 (2002) 59–74

EPSL

www.elsevier.com/locate/epsl

Major element heterogeneity in Archean to Recent mantle plume starting-heads

Sally A. Gibson *

Department of Earth Sciences, University of Cambridge, Downing Street, Cambridge CB2 3EQ, UK

Received 20 July 2001; received in revised form 17 October 2001; accepted 25 October 2001

Abstract

Variations in the bulk-rock compositions of primary high-Mg melts provide important constraints on the thermal and chemical structure of their mantle source regions. Picrites and komatiites of Archean to Recent age exhibit a wide range of FeO and Al_2O_3 at a given MgO content. Those with FeO* contents (total Fe as FeO) > 12.5 wt% have low Al_2O_3 contents (typically < 10 wt%), and also fractionated heavy rare-earth-element ratios ($[Gd/Yb]_n = 1.25–3.75$), that are consistent with melt generation in the garnet-stability field. The high-Fe magnesian melts typically have positive εNd values, which are similar or slightly lower than those of co-existing picrites and komatiites, and suggest that the convecting mantle was the predominant melt source region. The high-Fe magnesian magmas typically occur at, or close to, the base of igneous successions of Archean (e.g. Onverwacht Group, S. Africa and Superior Province, Canada) and Phanerozoic age (e.g. Siberia, Paraná-Etendeka, and the North Atlantic Igneous Province) and appear to represent some of the earliest magmas to be generated during melting of mantle plume starting-heads. Generation of high-Fe magnesian melts cannot be readily explained by high-pressure melting of fertile peridotite in a dynamic melting regime. A comparison of the bulk-rock compositions of Fe-rich picrites with the results of recent experimental studies on basalt–peridotite mixtures suggests that the high-Fe magnesian melts may have been generated by moderate amounts of partial melting of 're-fertilised' peridotite at potential temperatures of ≥1450°C and pressures ≥4.5 GPa. This hybrid Fe-rich peridotite is thought to result from a series of progressive mixing and reaction processes between subducted oceanic crust (eclogite) and convecting mantle. These findings suggest that compositional heterogeneity, involving streaks of recycled oceanic crust in a peridotite host, may have been a characteristic of mantle plume starting-heads since Archean times.

Keywords: picrite; komatiite; flood basalts; mantle plumes; eclogite; lithosphere

1. Introduction

Adiabatic decompression melting within the starting-heads of upwelling mantle plumes is widely believed to be responsible for the genesis of the enormous volumes of magma that constitute large igneous provinces. Those of Proterozoic and Phanerozoic age are dominated by low-MgO lavas with rare picritic (MgO > 12 wt%) flows, whereas Archean sequences typically contain komatiites (> 18 wt% MgO) and basaltic komatiites (18–12 wt% MgO). Variations in the bulk-rock compositions of these high-Mg melts have been

* Fax: +44-1223-333450.
E-mail address: sally@esc.cam.ac.uk (S.A. Gibson).

0012-821X/02/$ – see front matter
PII: S0012-821X(01)00566-0

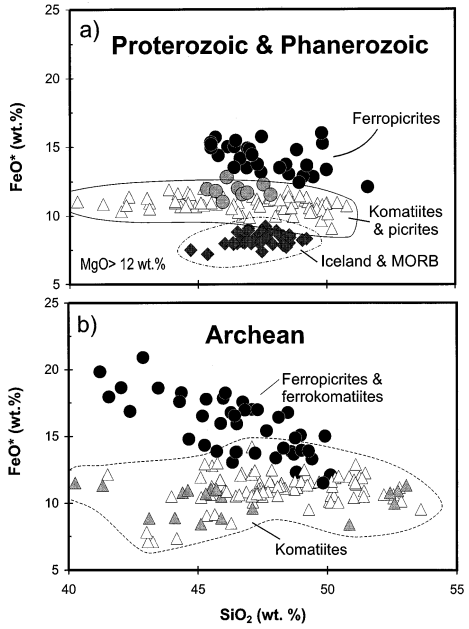

Fig. 1. Variation of SiO_2 and FeO* (total Fe) in Archean to Recent igneous rocks with >12 wt% MgO. Symbols are as follows: (a) Phanerozoic and Proterozoic: (black circles) ferropicrites (Paraná-Etendeka, Siberia, East Greenland, Deccan and Pechenga); (grey circles) Skye; and (white triangles) komatiites and picrites (Gorgona, Hawaii, West Greenland and Deccan). (b) Al-undepleted komatiites, (white triangles) Munro Township, Kambalda, Wawa, Belingwe and Lumby Lake; (grey triangles) Al-depleted komatiites, Onverwacht (Theespruit and Komati Fms); (black circles) Ferropicrites/ferrokomatiites, Onverwacht (Sandspruit and Schapenburg Fms), Wawa, Lake of the Enemy, Boston Township, Steep Rock, Lumby Lake and Kolar. Data sources are given in [7] with additional analyses from [1,13,18,19,30,31,47–59].

used to provide constraints on the thermal and chemical structure of their mantle source region(s). For example, the decrease in MgO contents of Archean to Recent melts is believed by some to indicate a secular decrease in: (i) depth of adiabatic decompression melting of mantle plumes [1–4]; and (ii) mantle potential temperature, which is thought to be $\sim$200°C lower at the present-day [5]. Nevertheless, uncertainty over the primary melt compositions of Archean komatiites, such as their MgO contents and hydrous versus anhydrous nature, limits our ability to constrain mantle temperatures and source compositions [6].

Phanerozoic continental flood-basalt (CFB) provinces lack the structural complexity and low-grade metamorphism that have proved problematic in interpreting komatiite petrogenesis, and may offer a key to understanding Archean and Early Proterozoic processes. A recent study of high-MgO magmas from Phanerozoic CFBs has revealed that they exhibit marked variations in their FeO* (total Fe) and Al_2O_3 contents, and rare-earth-element (REE) ratios, at a given MgO value [7]. Those with high FeO* are believed to have been generated by adiabatic decompression melting of Fe-rich streaks in upwelling mantle plume starting-heads, rather than by high-pressure (>6 GPa) melting of fertile peridotite [7]. Relatively high contents of FeO* are also characteristic of high-Mg melts in Archean and Proterozoic CFBs [8]. This paper examines the similarities in the bulk-rock compositions of Archean to Recent Fe-rich melts and the role of recycled oceanic crust in their genesis.

2. Phanerozoic anhydrous high-Mg melts

The generation of high-Mg anhydrous melts requires mantle potential temperatures that are $\sim$200°C in excess of those of ambient upper mantle [9,10]. Evidence for the existence of Phanerozoic primary high-Mg melts is preserved in picritic (>12 wt% MgO) lavas and hypabyssal intrusions in CFB provinces (e.g. Deccan, Greenland, Karoo, Paraná-Etendeka, British Tertiary), on oceanic islands (e.g. Hawaii, Iceland) and also and oceanic plateaux (e.g. Gorgona). On the continents, picritic rocks typically form a volumetrically minor proportion of lava piles; more significant quantities of these relatively high-density melts were probably trapped in magma chambers at the base of the crust.

Estimates of parental melt compositions of Phanerozoic picrites, based on analyses of olivine phenocrysts (up to Mg# = $\sim$92) range from $\sim$15 to 19 wt% MgO with Mg# = $\sim$0.75–0.79 (where Mg# = Mg/(Mg+Fe) (e.g. [11,12]). Most of the parental picrite melts are believed to have segregated from their mantle source regions between 4.5 and 2.0 GPa and at potential temperatures up to 1600°C [11,12]. Rare high-Mg# olivine phe-

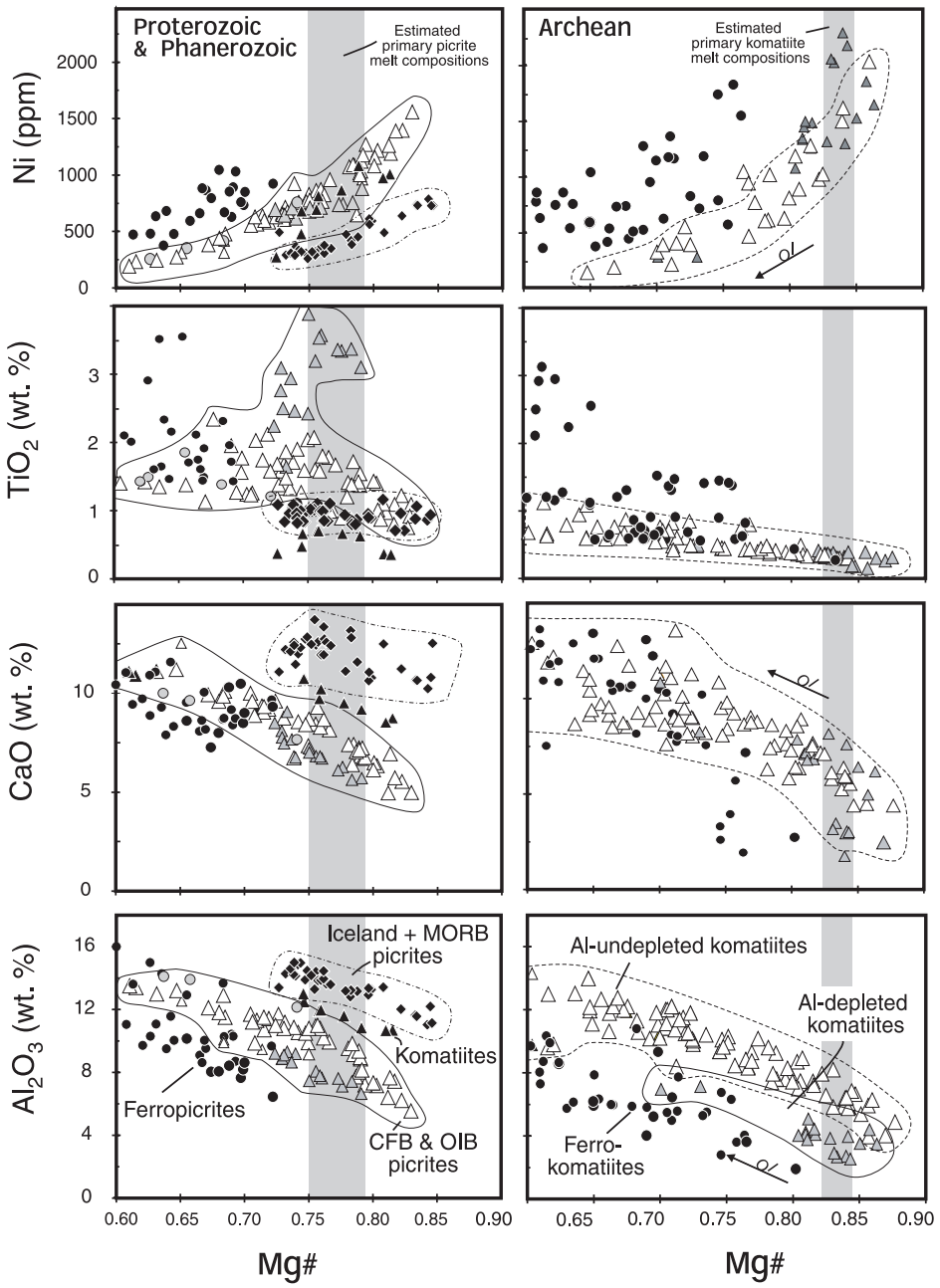

Fig. 2. Variation of Mg# with selected major and trace element abundances in Archean to Recent igneous rocks containing >12 wt% MgO. Mg# = Mg/(Mg+Fe^{2+}) and $Fe^{2+} = 0.9 \times Fe_{total}$ as discussed in the text. Symbols for Phanerozoic and Proterozoic rocks are: (white triangles) Hawaii, West Greenland and Deccan; (black triangles) Gorgona; (grey triangles) Karoo; (grey circles) Skye; (black circles) Paraná-Etendeka, Deccan, Siberia, East Greenland and Pechenga; (black diamonds) Iceland and South Atlantic MORB. Symbols for Archean rocks are: (white triangles) Munro Township, Kambalda, Wawa, Belingwe and Lumby Lake; (grey triangles) Onverwacht (Theespruit and Komati Fms); (black circles) Onverwacht (Sandspruit and Schapenburg Fms), Wawa, Lake of the Enemy, Boston Township, Steep Rock, Lumby Lake and Kolar. Vertical shaded regions illustrate the estimated Mg# of parental melts for picrites and komatiites. Vectors illustrate the effects of olivine fractionation. Data sources are the same as Fig. 1.

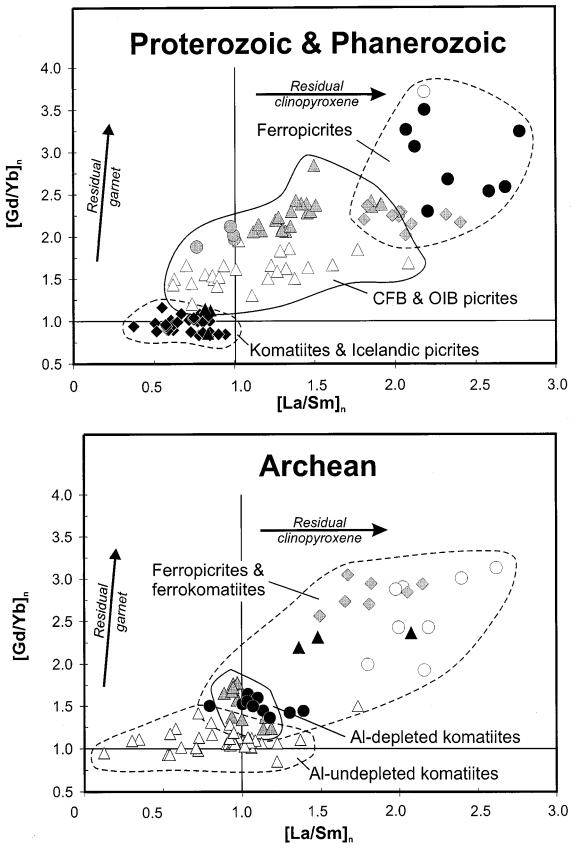

Fig. 3. Variation of chondrite-normalised REE ratios in Archean to Recent high-Mg igneous rocks. Vectors indicate the control of garnet and clinopyroxene in the melt source region. Bulk-Earth values of $[La/Sm]_n$ and $[Gd/Yb]_n$ are shown for reference. Data sources are given in Fig. 1. Symbols for Phanerozoic and Proterozoic rocks are: (grey triangles) Hawaii; (white triangles) West Greenland; (black triangles) Gorgona; (grey circles) Skye; (black circles) Paraná-Etendeka; (grey diamonds) Siberia; (white circles) East Greenland; (black diamonds) Iceland and South Atlantic MORB. Symbols for Archean rocks are: (white triangles) Munro Township, Kambalda, Wawa, Belingwe and Lumby Lake; (grey triangles) Onverwacht (Theespruit and Komati Fms); (black circles) Onverwacht (Sandspruit and Schapenburg Fms); (black triangles) Wawa; (grey diamonds) Lake of the Enemy; (white circles) Boston Township, Steep Rock and Lumby Lake.

nocrysts (up to 93.5) in Phanerozoic picrites from Baffin Island, West Greenland, Gorgona (Columbia) and the Paraná-Etendeka CFB, may be evidence of even higher mantle potential temperatures (1700°C) and greater depths (6 GPa) of adiabatic decompression melting in non-Newtonian mantle plumes [13]. Additionally, anhydrous, mildly to sub-alkaline picrites with anomalously high FeO* (>12.5 wt%), low Al_2O_3 and high $[La/Sm]_n$ (1.5–3) and $[Gd/Yb]_n$ ratios (2–3.5; Figs. 1–3) may be evidence of compositionally heterogeneous Phanerozoic mantle plumes [7].

2.1. Phanerozoic and Proterozoic ferropicrites

The term 'ferropicrite' was first used by Hanski and Smolkin [14] to describe Early Proterozoic high-FeO* (14.8–18 wt%) picrites from Pechenga, NW Russia. More recently their occurrence has been noted near the base of several Phanerozoic CFB successions ([7]; Fig. 4). Examples include: (i) Tertiary East Greenland Lower Basalts (Mikis Fm [15]); (ii) the Early Cretaceous Paraná-Etendeka CFB (Awahab Fm [7]); and (iii) the Permo–Triassic Siberia CFB (Gudchikhinsky Fm [16,17]). Picrites and basalts higher up in these successions lack the anomalously high-Fe contents. Fe-rich picrites are also present in the Deccan CFB in the Poladpur and Thakurvadi Formations [18,19].

The major element geochemistry of the ferropicrites is dominated by high-pressure (~ 0.9 GPa) crystallisation of olivine, clinopyroxene and plagioclase feldspar [7,14]. Trace element ratios (e.g. $[La/Nb]_n \sim 1$) and radiogenic isotopes (εNd usually >0; Fig. 5) of many ferropicrites are similar to those of OIB (ocean–island basalts) and indicate that most of the parental magmas have only undergone limited crustal contamination. The anhydrous mineral assemblage of the unaltered ferropicrites, combined with relatively low alkali contents and LREE ratios (e.g. $[La/Sm]_n = 1.5–3$; Fig. 3) preclude significant melt contributions from metasomatised lithospheric mantle.

2.1.1. Estimation of parental ferropicrite melt compositions

Fresh olivine phenocrysts have been observed in ferropicrites from East Greenland [14], Paraná-Etendeka [7] and Pechenga [14]. These are characterised by low Mg# (<0.86) relative to olivine phenocrysts from other picrite and komatiite suites (Fig. 5). Despite this, the ferropicrite olivines have high NiO (up to 0.6 wt%) and Cr_2O_3 contents (up to 0.1 wt%, Fig. 6). These

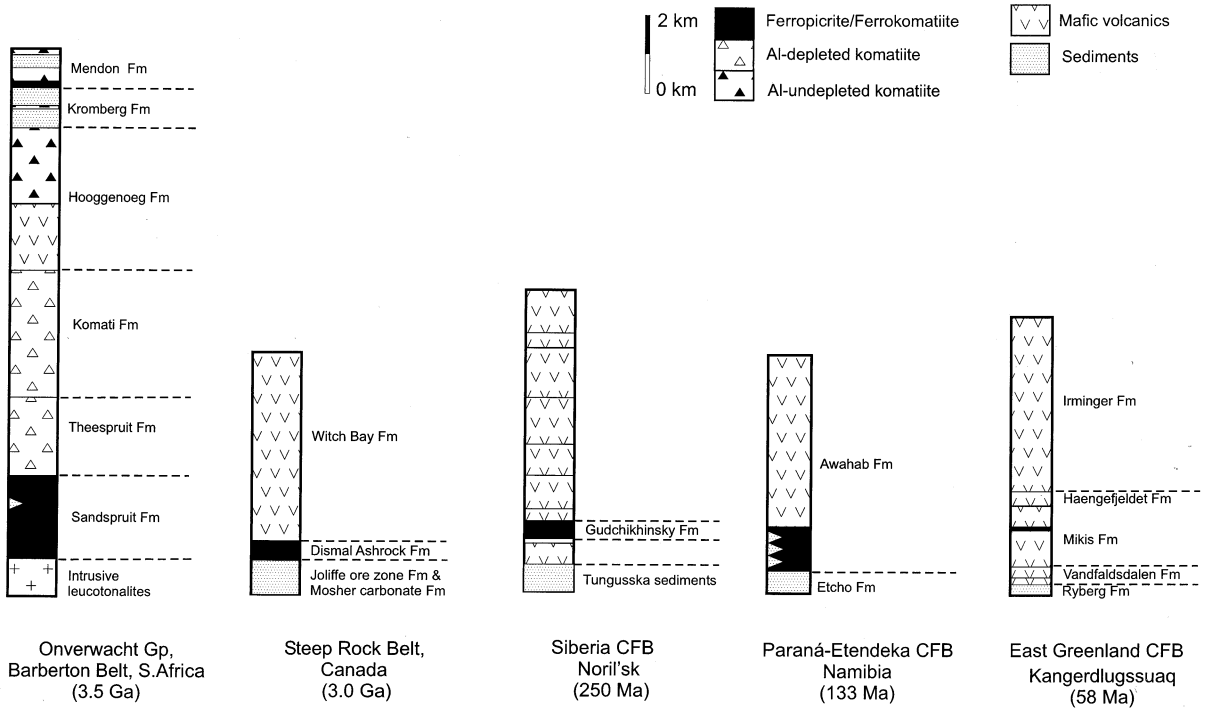

Fig. 4. Stratigraphic location of high-Fe magnesian rocks in Archean to Recent large igneous provinces. Note the occurrence of the high-Fe picrites/komatiites at or near the base of the successions and also their relatively low volume of the total magmatism. Stratigraphic successions are modified from [17,31,61–63].

are comparable to those of olivine phenocrysts in picrites from CFB provinces and ocean islands. Using $K_{D\,Ni}^{Ol-liquid}$ and $K_{D\,Cr}^{Ol-liquid}$ values of 6.4 and 0.6, respectively [20,21], the ferropicrite olivines (Fo_{86}) are estimated to have equilibrated with melts containing ~680 ppm Ni and ~1140 ppm Cr.

In order to calculate the Mg# of the parental ferropicrite melt it is necessary to estimate the Fe_2O_3/FeO ratio. This is usually assumed to be a ratio of 0.1 but it is clearly important to justify this for rocks with anomalously high FeO*. The oxygen fugacity of the ferropicrite magma has been estimated on the basis of $Mg^{2+}$and Fe^{2+} exchange between co-existing olivines and spinels [22]. Since Mg/Fe ratios are affected by hydrothermal alteration, it has only been possible to estimate $\Delta\log fO_2$ values for the Paraná-Etendeka ferropicrites. These fall between the fayalite–magnetite–quartz (FMQ) and iron–wustite buffers and range from −1.36 to −4 $\Delta\log fO_2$ units below FMQ. These estimates are consistent with those predicted from the Cr_2O_3 contents (0.06 ± 0.026 wt%) of ferropicrite olivine phenocrysts (Fig. 7). The lowest estimates of temperature and fO_2 values on Fig. 7 probably reflect cationic diffusion of Mg and Fe during cooling. In this study it is assumed that the spinel–olivine pair with the highest calculated ΔfO_2 has undergone the least subsolidus re-equilibration; the Fe_2O_3/FeO ratio estimated for the ferropicrites will therefore be a minimum value. Using the empirical expression of Kilinc et al. [23] with the revised coefficients of Holloway et al. [24], and the highest calculated olivine–spinel equilibration temperature and fO_2, the estimated Fe_2O_3/FeO ratio of the ferropicrite magma ranges from 0.1 to 0.08. Using an Fe_2O_3/FeO ratio of 0.1 and a $K_{D\,Fe-Mg}^{Ol-liquid}$ of 0.32 [25], the estimated Mg# of the Paraná-Etendeka ferropicrite parental melt is ~0.66. This closely corresponds with the bulk-rock Mg# of the Paraná-Etendeka ferropicrites and also some of the East

Greenland and Pechenga samples (Table 1). Others, with higher Mg# and Ni contents, may have accumulated olivine phenocrysts. Fig. 8 shows that some of the Pechenga and Siberia ferropicrites may have accumulated up to ~15% olivine (Fo_{86}) but this has not affected their bulk-rock FeO contents.

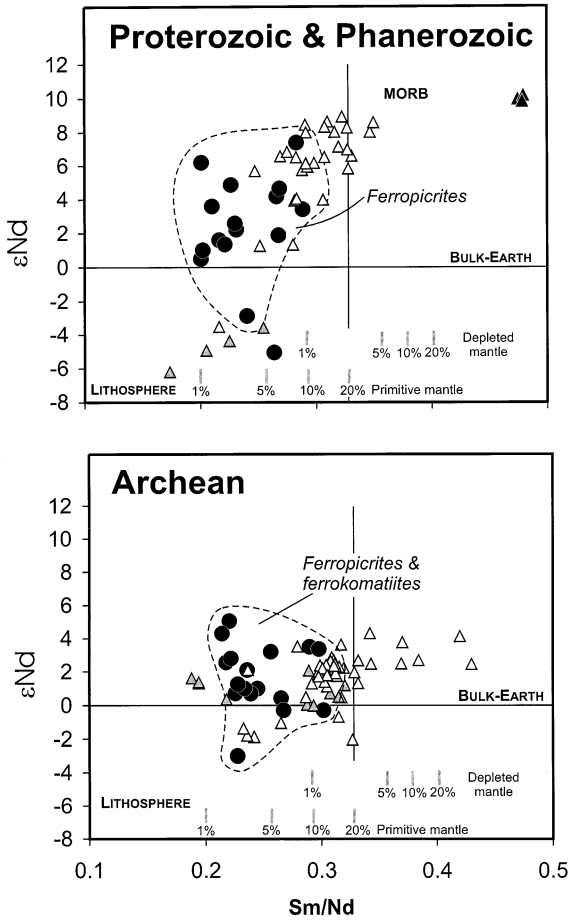

Fig. 5. Variation of Sm/Nd ratios with εNd values in Archean to Recent high-Mg igneous rocks. Bulk-Earth, MORB and ancient lithosphere are shown for comparison. Note that almost all of the high-Fe magmas are characterised by relatively low Sm/Nd ratios and positive εNd values. The vertical bars indicate Sm/Nd ratios in liquids produced by 1–20% partial batch melting of depleted and primitive mantle in which Sm/Nd = 0.37 and 0.32, respectively [60]. The low Sm/Nd ratios of the high-Fe picrites and komatiites require, despite their depleted isotopic ratios, that a melt source region more enriched in light REE than depleted mantle contributed to their genesis. Data for high-Mg igneous rocks are from references provided in Fig. 1 and symbols are the same as for Fig. 2.

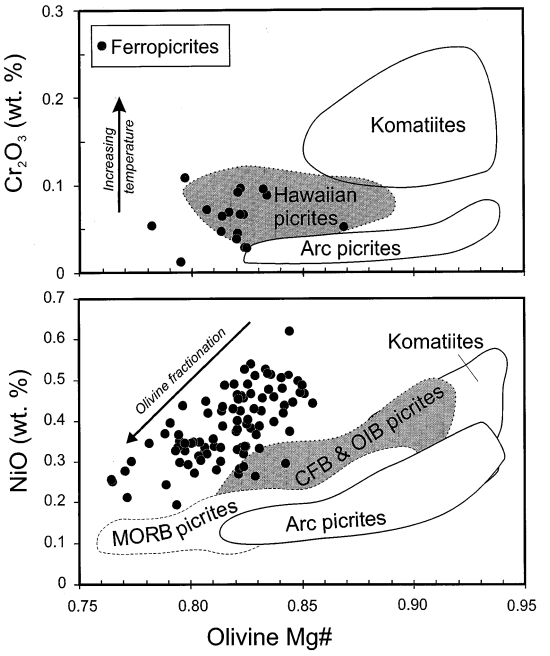

Fig. 6. Variation of Mg# with Cr_2O_3 and NiO in olivines from high-Mg igneous rocks. The high Cr_2O_3 contents of komatiite olivines are believed to be due to high crystallisation temperatures rather than unusually low fO_2 conditions [64]. Crystal fractionation of olivine causes a decrease in both Mg# and NiO and therefore cannot be responsible for the relatively low Mg# but high NiO of the ferropicrite olivines. Data are from Table 1, the author's unpublished data set and [7,65–70].

3. Archean high-Mg melts

Confirmation that Archean komatiites have an origin associated with mantle plumes is provided by their high $^3He/^4He$ ratios (up to 39 R/R_a [26]). Nevertheless, the origin of their parental melts remains controversial. Fundamental differences are thought to exist in the melt generation histories of so-called 'Al-depleted' and 'Al-undepleted' komatiites. Herzberg [27] and Nisbet et al. [3] proposed that the Al-depleted komatiites, which predominantly occur in 3.4 Ga igneous successions (e.g. Onverwacht Group, South Africa and Pilbara, Australia), were generated at higher man-

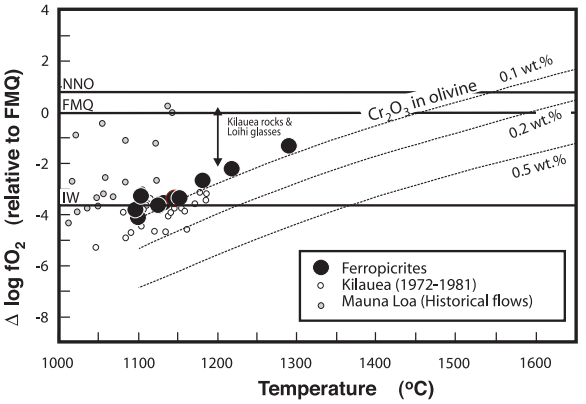

Fig. 7. Estimates of oxygen fugacity (fO_2) and temperature from microprobe analyses of olivine–spinel pairs in Paraná-Etendeka ferropicrites (Table 1). Oxygen fugacities and temperatures were calculated using the method of [21]. SiO_2 activities were estimated from [71] and Δlog FMQ values were calculated using the equation of [72]. Isopleths for Cr_2O_3 contents in olivine are also shown [64]. The calculated oxygen fugacities and temperatures are consistent with Cr contents that reach up to 0.1 wt% in ferropicrite olivines (Table 1). Temperatures and oxygen fugacities calculated for olivine–spinel pairs from Kilauea (white circles; Table 1, [73]) and Mauna Loa (grey circles; Table 1, [69]) are also shown. The similar higher ΔfO_2 values for glasses and rocks from Kilauea and Loihi, relative to estimates from olivine–spinel pairs, illustrate the effects of cationic diffusion during chromite re-equilibration [73].

tle potential temperatures and pressures than 'Al-undepleted' komatiites which dominate 2.7 Ga sequences (e.g. Munro Township, Canada and Belingwe Belt, Zimbabwe). Other workers have suggested that the variations in Al_2O_3 contents may also result from source heterogeneity, e.g. [28].

The highly magnesian olivines present in both Al-depleted and Al-undepleted komatiites (Mg# = up to 0.94) require that they were in equilibrium with liquids containing very high-MgO contents (~29 wt% [3]). Similarly, estimates of Mg# for Archean mantle melts are considerably higher (~0.84) than those for Proterozoic and Phanerozoic melts (0.75–0.79). This secular variation in MgO has been interpreted by some as evidence for anhydrous melting at significantly higher mantle potential temperatures (up to 1900°C) in the Archean [3,27]. Others have invoked that these high-MgO liquids may be produced by hydrous melting of fertile lherzolite but, there is currently no compelling published evidence that significant quantities of H_2O existed in komatiite melt source regions (see discussion in [6]).

3.1. Archean ferropicrites/ferrokomatiites

In addition to the Al-undepleted and Al-depleted variants of komatiites, there also appears

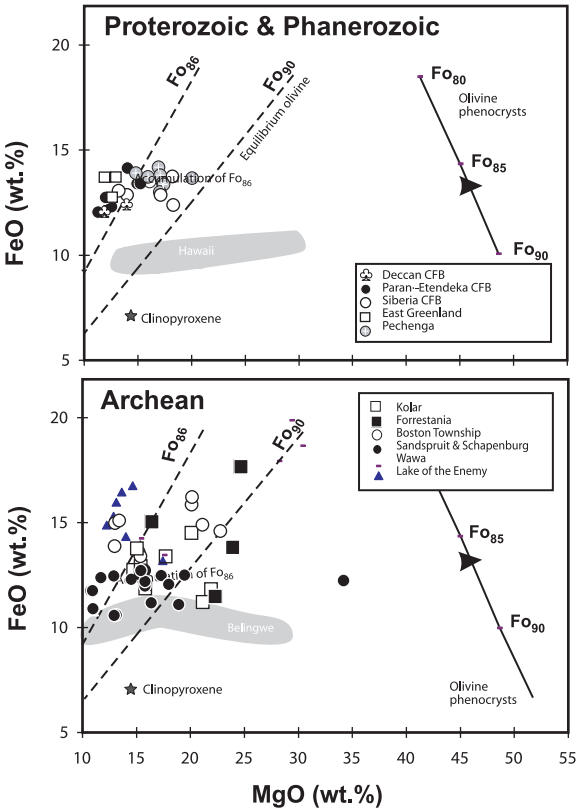

Fig. 8. Variation of MgO and FeO in Archean to Recent high-Fe magnesian magmas. Picrites from Hawaii and komatiites from Belingwe are shown for comparison. The dashed lines illustrate the composition of melts in equilibrium with Fo_{86} and Fo_{90} assuming 0.1% Fe_2O_3 (see text for discussion). A liquid in equilibrium with Fo_{xx} (where xx is the forsterite content) should plot at the intersection of the Fo_{xx} dashed line and the corresponding olivine control line. The observed olivine control line in the ferropicrites shows that some of the rocks may have accumulated up to ~15% of Fo_{86}. A similar control line has been plotted for the Archean samples; this is for comparative purposes only as there are no reported occurrences of fresh olivine in these rocks. Data sources are the same as Fig. 1.

Table 1
Comparison of bulk-rock compositions of Archean to recent high-Fe magnesian magmas with the result of an experimental study on basalt–peridotite mixtures

		Archean					Proterozoic	Phanerozoic			
Age (Myr):	Conditions[c]	3400	2900	2700	2700	2700	1900	250	132	65	60
Location:		Onverwacht	Kolar	Lake of the Enemy	Wawa	Boston Township	Pechenga	Siberia	Paraná-Etendeka	Deccan	East Greenland
Sample No:		SC19	18-10	EN3	SC96-8	I-J29	PCH1	SG-32 2332	96SB48	ABC29	GM20332
SiO_2	45.90	48.70	45.33	46.49	47.08	48.96	49.84	48.17	46.14	46.87	48.52
TiO_2	1.80	0.58	1.28	2.55	0.87	0.70	2.26	1.49	1.91	1.39	2.11
Al_2O_3	11.70	6.34	11.86	7.88	10.80	4.03	8.05	10.32	9.52	10.79	11.15
Fe_2O_3	13.89	15.20	14.27	17.70	15.80	16.79	16.96	14.99	16.70	15.09	14.15
MnO	0.20	0.27	0.21	0.27	0.23	0.18	0.19	0.17	0.19	0.19	0.15
MgO	16.50	14.50	15.06	14.13	15.40	15.22	15.95	16.10	15.39	12.01	12.67
CaO	8.40	12.10	10.52	12.09	8.17	13.09	7.26	8.74	8.18	11.32	9.24
Na_2O	2.10	1.40	0.68	0.37	0.95	0.55	0.23	1.24	2.03	1.71	1.84
K_2O	0.50	0.14	0.06	0.07	0.63	0.04	0.25	0.07	0.63	0.45	0.34
P_2O_5	0.20	0.06	–	0.23	0.09	0.01	0.22	0.14	0.17	0.13	0.22
Cr_2O_3	0.20	0.00	0.00	0.00	0.00	0.00	0.00	0.00	0.00	–	0.00
NiO	–	0.00	0.00	0.00	0.00	0.00	0.00	0.00	0.00	0.00	0.00
Total	101.19	99.29	99.27	101.78	100.02	99.57	101.21	101.43	100.86	99.95	100.39
LOI	–	0.76	–	1.17	1.06	3.28	4.82	7.79	0.22	–	3.14
Mg#	0.70	1.00	1.00	1.00	1.00	1.00	1.00	1.00	1.00	1.00	1.00
Fo_{max}	84.5	86[a]	–	–	–	85.5[b]	85	–	86	–	84

Where Mg# = atomic Mg/(Mg+Fe) and $Fe^{2+} = 0.9 \times$ total Fe. Fo_{max} is the maximum Mg/(Mg+Fe) of olivine analysed or estimated for a given suite of rocks. Data sources are [7,8,15,17,19,34,41,55,57,58,74].

[a] Estimated from Fig. 8.

[b] Estimated in [74].

[c] 1500°C, 3.5 GPa, 50% GA, 50% MPY.

to be another distinct variety that is Al-depleted and rich in FeO* (ferrokomatiites). The occurrence of high-Fe basaltic komatiites was first noted in the Vermillion Belt of Minnesota [29]. Other examples occur at the base of the 3.4 Ga Onverwacht Group (Sandspruit and Schapenburg Fms) and the 3.0 Ga Steep Rock Group (Dismal Ashrock Fm). They are also present in 3.0 to 2.7 Ga komatiite successions in: the Steep Rock, Wawa and Abitibi Belts in the Superior Province (Canada); the Kolar Schist Belt (India) and the Forrestania Belt (Australia). These rocks are distinguished from other Al-depleted komatiites (e.g. Komati and Theespruit Fms, Onverwacht Group), by their very high contents of FeO* (up to 20 wt%; Fig. 1) and TiO_2 (up to 3.5 wt%), fractionated HREE ($[Gd/Yb]_n = 1.7–3$) and relatively high LREE ratios ($[La/Sm]_n = 1–2.5$; Fig. 3). Linear variations between bulk-rock MgO and FeO (Fig. 8) suggest that the composition of the high-Fe picrites/komatiites is controlled by the accumulation of olivine which is considerably more Fe-rich ($< Fo_{90}$) than that in komatiites. In many respects, the compositional variations exhibited by the Archean high-Fe magnesian melts are similar to those of the Proterozoic and Phanerozoic ferropicrites described above.

Interpretations of the petrogenesis of these Archean high-Fe magnesian rocks are enigmatic, primarily because all reported occurrences have undergone greenschist- or amphibolite-facies metamorphism. Most of the high-Fe picrites/komatiites have positive εNd values (up to +6, Fig. 5). These positive values, together with low La/Nb ratios, suggest that the bulk-rock compositions of the high-Fe magnesian magmas are relatively unaffected by crustal contamination. Their incompatible trace element ratios are therefore assumed to be a consequence of partial melting of their mantle source region(s). The 2.7 Ga Abitibi Belt (Boston Township) and 3.0 Ga Steep Rock Belt high-Fe picrites/komatiites have attracted attention because of their exceptionally high CaO/Al_2O_3 and strongly fractionated HREE ratios (Fig. 9). Both of these element ratios are increased if garnet is present as a residual phase during melting and the high-Fe melts have been variably interpreted as:

1. Ultra-high-pressure melts (> 14 GPa) of fertile lherzolite in super-hot plumes [4,30,31];
2. Melts of a recycled subduction-related component entrained within a mantle plume [32].
3. The products of melting of 'solidified komatiite' at 4 GPa that had initially been generated by partial melting of fertile peridotite at high pressures (~ 10 GPa [33]).

Fig. 9 shows that there is a large variation in CaO/Al_2O_3 ratios in world-wide Archean high-Fe magnesian magmas (0.3 to > 2). In contrast, Phanerozoic ferropicrite CaO/Al_2O_3 ratios are almost constant (average = 0.85, $1\sigma = 0.15$), and slightly lower than estimates for primitive mantle (average = 0.93 [4]). Those with high CaO/Al_2O_3 also have high loss-on-ignition values. The large variations in CaO/Al_2O_3 ratios at a given $[Gd/Yb]_n$ ratio (Fig. 9), and also wide range of $[La/Sm]_n$, exhibited by the Archean high-Fe picrites/komatiites, suggest that their CaO/Al_2O_3 ratios do not simply reflect the amount of residual garnet in the mantle source region. The wide variation in CaO/Al_2O_3 ratios in the komatiites is predominantly due to the mobility of CaO during alteration and is not a useful ratio in assessing melting processes.

4. Generation of high-Fe mantle melts

Similarities in bulk-rock compositions of Archean, Proterozoic and Phanerozoic high-Fe magnesian magmas (Figs. 1, 2 and 5) imply that their parental melts were generated from comparable melting regimes. At a given SiO_2 content, the average FeO* content of these samples is > 3 wt% more than OIB and > 6 wt% higher than MORB, (Fig. 1). These and other variations in elemental concentrations between the high-Fe magnesian magmas and picrites/komatiites cannot be readily explained by crystal fractionation. They require that their primary melts were generated by either: (i) different degrees of partial melt-

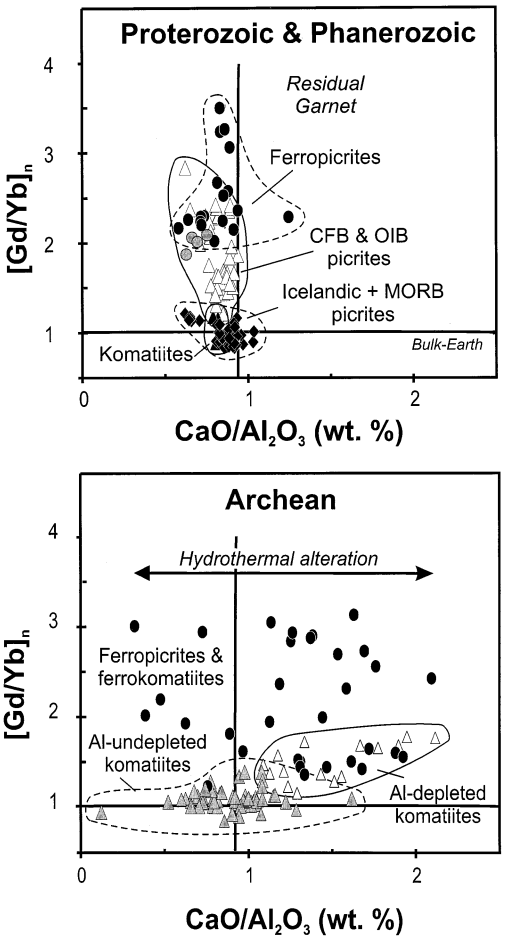

Fig. 9. Variation of CaO/Al_2O_3 and $[Gd/Yb]_n$ in Archean to Recent high-Mg igneous rocks. The average CaO/Al_2O_3 and $[Gd/Yb]_n$ ratios of primitive mantle are shown for comparison [4,58]. Data sources are the same as Fig. 1 and symbols are the same as Fig. 2.

ing and/or (ii) from different mantle source regions.

4.1. Hydrous or anhydrous melts?

Hanski and Smolkin [34] have proposed that the Early Proterozoic Pechenga ferropicrites crystallised from hydrous magmas. Their interpretation is based on the presence of kaersutite, which occurs both as reaction rims around spinifex pyroxenes, and also as an interstitial phase (together with phlogopite) in a chloritic mesostasis. Unlike the Pechenga rocks, the Early Cretaceous Paraná-Etendeka and Tertiary East Greenland ferropicrites have not undergone hydrothermal alteration or greenschist-facies metamorphism and there is no uncertainty regarding the primary origin of their constituent mineral phases. There is no petrographic or geochemical evidence to indicate that the Phanerozoic ferropicrites were derived from 'wet' magmas; they do not contain hydrous phenocrysts and some have very low loss-on-ignition values (<0.5 wt%). Paradoxically, the Proterozoic and Phanerozoic ferropicrites have almost identical bulk-rock compositions (Table 1). The only elements that exhibit variations between these two suites are those which are notoriously susceptible to hydrothermal alteration, e.g. CaO, Sr, Ba, Rb and K. Since experimental melts of hydrous peridotite are characterised by low FeO* contents, relative to dry equivalent melts at the same pressure [35], it seems unlikely that the high-Fe content of the high-Fe magnesian melts are due to melting of a 'wet' mantle source. In cases where hydrous phases have been observed [34,36] the parental magmas may have interacted with water prior to, or during, crystal fractionation.

4.2. Eclogite and/or peridotite mantle source?

It has long been recognised that the MgO and FeO contents of mantle melts increase as the pressure at which the upwelling peridotite intersects the solidus increases. Dynamic melting models have therefore been proposed to account for variations of FeO in individual suites of mantle-derived melts [37]. High-pressure melting of a peridotite source can not, however, explain the high TiO_2 contents of the high-Fe magnesian melts (Fig. 2). An alternative way of generating FeO-rich melts is by partial melting of a pyroxene-rich (e.g. eclogite or websterite) mantle source. This material may be present in the convecting mantle in significant amounts as (i) subducted oceanic crust and/or (ii) recycled Fe-rich mafic residues that formed during growth of granitic crust. Evidence for the presence of subducted oceanic lithosphere in the lower mantle is provided by high-resolution seismic tomography studies (e.g. [38]). Accumulation of this material at the core mantle

boundary and subsequent entrainment by mantle plumes may explain the isotopic and trace element variations in OIBs. Nevertheless, it is unclear as to how much this recycled oceanic and/or continental crust contributes to the major element heterogeneity of plume-derived melts.

The solidus temperatures of recycled oceanic crust would be lower than those of the surrounding peridotite whereas recycled Fe-rich mafic cumulates would melt at similar or higher temperatures than the peridotite. These differences would influence the timing of the emplacement and eruption of the Fe-rich melts. Since the high-Fe melts predominantly occur at the base of volcanic successions, it is assumed that they are generated from a source with a low melting temperature relative to the surrounding peridotite, i.e. recycled oceanic crust.

Using the results of new experimental studies, Cordery et al. [39] and Takahashi et al. [40] suggested that CFB's may result from partial melting of eclogite streaks in upwelling mantle plumes. The results of these experimental studies show that eclogite partial melts are rich in SiO_2, Al_2O_3, FeO and Na_2O. Nevertheless, they have relatively low MgO contents and melting of such a mantle source, alone, could not generate the high-Fe picrite/komatiite parental melts. Furthermore, the high Ni contents of the high-Fe magnesian melts require that they were derived, at least in part, from a peridotite mantle source. One explanation for their unusually high-Fe contents is that they are partial melts of hybrid basalt–peridotite bulk-rock compositions.

Yaxley and Green [41] undertook a series of experiments on peridotite/eclogite mixtures. They found that at 3.5 GPa and $\sim$1300°C, the eclogite melts and reacts with olivine in the surrounding peridotite to form orthopyroxene and garnet. Further melting of the residual eclogite produces andesitic partial melts that react with the surrounding peridotite and enrich it in garnet and clinopyroxene. Melting of this 're-fertilised' peridotite produces picritic liquids whose major element concentrations are controlled by the degree of partial melting and the modified bulk-rock composition. This anhydrous 're-fertilised' peridotite is relatively Fe-rich and the preferred melt source region for the high-Fe picrites/komatiites. Small-fraction melts of the re-fertilised peridotite are Ne-normative but become Hy-normative at higher melt fractions and lower pressures [41]. At a given degree of partial melting, melts derived from this Fe-rich peridotite mantle source will have higher $[Gd/Yb]_n$ and $[La/Sm]_n$ ratios than those from 'normal' peridotite due to the higher proportions of garnet and clinopyroxene in the former.

4.3. Depth and extent of melting

The depth at which the mantle solidus is encountered depends on both composition and temperature [9]. The extent of subsequent adiabatic decompression melting is predominantly controlled by the thickness of the overlying lithosphere [10], which provides a physical barrier to mantle upwelling. The high $[Gd/Yb]_n$ ratios and low Al_2O_3 contents of the high-Fe picrites/komatiites are consistent with high-pressure melting and the presence of residual garnet in their melt source regions.

Fig. 10 shows the solidus curves for eclogite [43], fertile peridotite [44] and Fe-rich 're-fertilised' peridotite. The latter is believed to be $\sim$50°C below the solidus of fertile peridotite at a given pressure [41,42,45]. At the potential temperatures (T_{ps}) estimated for Phanerozoic mantle plumes (1450 to 1600°C), the eclogite solidus will be intersected at pressures $>$6.2 GPa. Ephemeral eclogite-derived melts will react with the surrounding peridotite and enrich it in Fe, Na and incompatible trace elements [45]. Subsequent adiabatic decompression melting will continue until the eclogite source is exhausted; 'streaks' of this recycled oceanic crust are believed to have thicknesses of metres to kilometres [46] and may be completely melted before the upwelling mantle encounters the base of the overlying lithosphere. During plume upwelling, the solidus of the 're-fertilised' peridotite will be intersected at $>$4.5 GPa (Fig. 10) and Fe-rich picritic melts will be generated. The aggregate melt fractions that result from subsequent adiabatic decompression melting will have higher FeO contents than those predicted by the experimental studies of Yaxley and

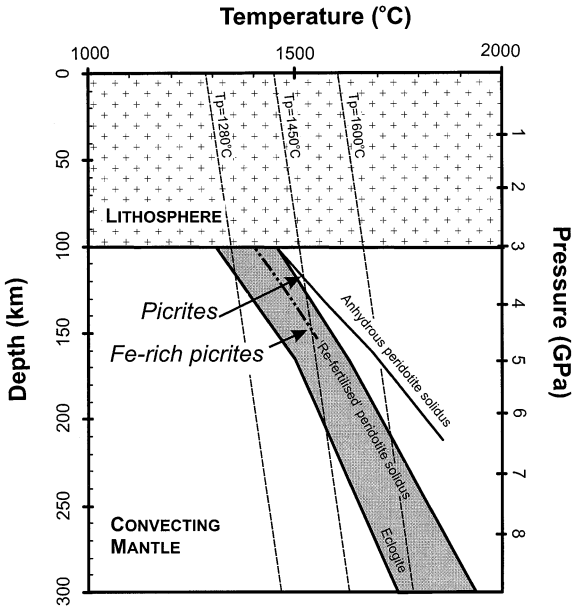

Fig. 10. *P–T* plot showing solidi for anhydrous fertile peridotite [44], 're-fertilised' peridotite [41], and eclogite [43]. Mantle adiabats for T_{ps} of Phanerozoic ambient mantle (1280°C) and mantle plumes (1450–1600°C) and a representative mechanical boundary layer thickness for the continental lithosphere are also shown.

Green [41], which are isobaric batch melts. Furthermore, the initial melts will be generated at higher pressures than those used in the experiments (3.5 GPa) and this may account for the lower contents of Al_2O_3 in the ferropicrites relative to hybrid basalt–peridotite melts (Ga1MPY90; Table 1). The degree of interaction of eclogitic melts with the surrounding mantle depends on the processes involved in melt migration and extraction, which are poorly understood. At T_{ps} of 1600°C and 1450°C anhydrous fertile peridotite will begin melting at 5.7 and 3.5 GPa, respectively. Melts derived from this source will dilute the effects of the eclogite heterogeneities, especially if the overlying lithosphere is relatively thin (<100 km) and allows a large amount of adiabatic decompression melting.

Following the initial impact of a mantle plume starting-head, melts are generated at progressively shallower depths with much of the melting occurring between 4 and 1.5 GPa. If the model outlined above is correct, then melts predominantly derived from the 're-fertilised' peridotite will be generated at the leading edge or margins of the plume starting-head where the temperatures are relatively low. This is consistent with the occurrence of high-Fe magnesian rocks near the base of CFB successions. High degrees of partial melting, associated with higher mantle potential temperatures within the core of the upwelling mantle plume (Fig. 11), will overprint the signatures of melts derived from the 're-fertilised' mantle.

The temperatures of Archean mantle plumes are believed to have been $\sim$200°C hotter than those in the Phanerozoic [3–5]. Initial melting of recycled oceanic crust entrained within Archean mantle plumes would therefore occur at much higher pressures (Fig. 11) and generate melts that were more depleted in Al_2O_3 (Fig. 2). The apparent absence of anhydrous Fe-rich magnesian melts in Phanerozoic OIB and MORB settings may be due to the large melting interval between the peridotite solidus and base of the lithosphere. This would enable considerable dilution of high-Fe 're-fertilised' mantle-derived melts by large-fraction peridotite-derived melts.

5. Conclusions

Archean to Recent anhydrous high-Mg melts display a wide variation in bulk-rock FeO* at a given MgO content. Evidence that the high-Fe magnesian melts were generated by processes linked with mantle starting-plumes is provided by: (i) their spatial and temporal association with large igneous provinces; and (ii) the high mantle potential temperatures that are inferred from their bulk-rock compositions [7]. The occurrence of high-Fe magnesian magmas near the base of voluminous igneous successions (Fig. 4) implies that their parental melts were generated by melting of fusible material at the leading edge or margins of a mantle plume (Fig. 11). Low Al_2O_3 contents and high $[Gd/Yb]_n$ ratios suggest that the high-Fe melts were generated at either (i) higher pressures and/or (ii) from more garnetiferous source regions than temporally and spatially associated picrites and komatiites. This relationship is most readily explained by melting of recycled oce-

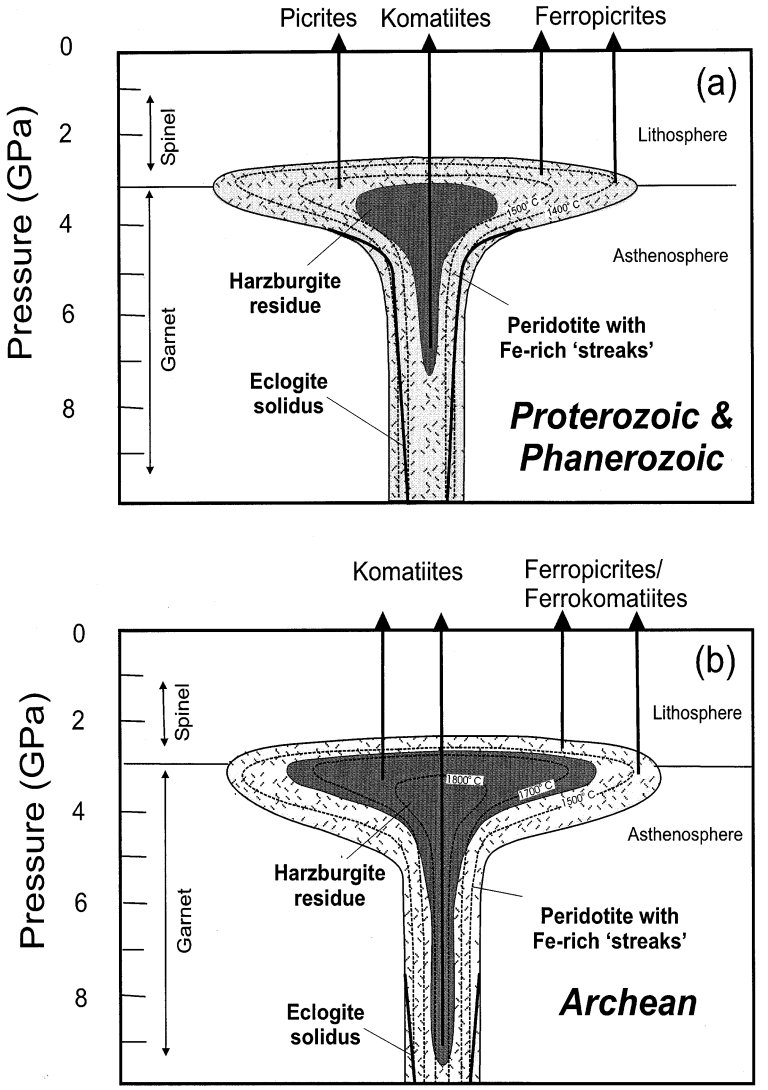

Fig. 11. Schematic illustrations to show the simplified thermal and compositional structure of (a) Archean, and (b) Proterozoic and Phanerozoic mantle plume starting-heads. Isotherms are labelled with potential temperature in degrees Celsius. The earliest melts to form are the high-Fe picrites/komatiites. These are derived from Fe-rich ('re-fertilised') peridotite 'streaks' at the leading edge and margins of the starting-plume-head. Subsequent melts are generated by larger degrees of partial melting at higher mantle potential temperatures. The eclogite solidus is from [43].

anic crust in an upwelling mantle plume. These eclogite 'streaks' would have lower solidi than the surrounding peridotite, enabling them to preferentially melt and react with their host. Subsequent melting of this 're-fertilised' peridotite would occur at $\sim$50°C below the 'normal' peridotite solidus and would be most easily identified at low-melt fractions. Progressive melting during upwelling of the mantle plume would generate melts from 'normal' peridotite. In regions of relatively thin lithosphere ($<$100 km), relatively large-fraction melts may dilute the signature of melts derived from the 're-fertilised' mantle source. The greater degrees of partial melting, that are inferred from the high-MgO combined with low Al_2O_3 and high $[Gd/Yb]_n$ ratios of

some 3.5 to 2.7 Ga high-Fe magnesian melts, are consistent with the higher potential temperatures that have been postulated for Archean mantle plumes (e.g. [5]).

The above conclusions concur with previous models that propose: (i) a secular decrease in mantle potential temperatures since the Archean [3,5,42] and (ii) heterogeneity in the mantle source regions of komatiites and picrites [7,28]. The presence of Fe-rich high-Mg rocks ranging from 3.5 Ga to 60 Ma in age (Table 1) does not, however, agree with models that invoke a marked decrease in the Fe content of the Earth's mantle since the Archean [8].

Acknowledgements

This work emanates from fieldwork and numerous enlightening discussions on magma genesis with Bob Thompson. The manuscript has benefited from detailed reviews by Nick Arndt, Ian Campbell and Don Francis. I am especially grateful to Ian Campbell for sharing his unpublished thoughts on picrite genesis. Support for this research was provided by the University of Cambridge. This is a Department of Earth Sciences, University of Cambridge contribution no. 6526.*[AH]*

References

[1] B. Jahn, G. Gruau, A.Y. Glikson, Komatiites of the Onverwacht Group, S. Africa; REE geochemistry, Sm/Nd age and mantle evolution, Contrib. Mineral. Petrol. 80 (1982) 25–40.

[2] G. Gruau, C. Chauvel, N.T. Arndt, J. Cornichet, Aluminum depletion in komatiites and garnet fractionation in the early Archean mantle; hafnium isotopic constraints, Geochim. Cosmochim. Acta 54 (1990) 3095–3101.

[3] E.G. Nisbet, M.J. Cheadle, N.T. Arndt, M.J. Bickle, Constraining the potential temperature of the Archaean mantle: a review of the evidence from komatiites, Lithos 30 (1993) 291–307.

[4] C. Herzberg, Generation of plume magmas through time; an experimental perspective, Chem. Geol. 126 (1995) 1–16.

[5] F.M. Richter, A major change in the thermal state of the Earth at the Archean-Proterozoic boundary: consequences for the nature and preservation of continental lithosphere, J. Petrol. Spec. Lithosphere Issue (1988) 39–52.

[6] N.T. Arndt, C. Ginibre, C. Chauvel, F. Albarède, M. Cheadle, C. Herzberg, G. Jenner, Y. Lahaye, Were komatiites wet?, Geology 26 (1998) 739–742.

[7] S.A. Gibson, R.N. Thompson, A.P. Dickin, Ferropicrites: geochemical evidence for Fe-rich streaks in upwelling mantle plumes, Earth Planet. Sci. Lett. 174 (2000) 355–374.

[8] D. Francis, J.R. Ludden, W. Davis, Picrite evidence for more Fe in Archean mantle reservoirs, Earth Planet. Sci. Lett. 167 (1999) 197–213.

[9] A.L. Jaques, D.H. Green, Anhydrous melting of peridotite at 0–15 kbar pressure and the genesis of tholeiitic basalts, Contrib. Mineral. Petrol. 73 (1980) 287–310.

[10] D. McKenzie, M.J. Bickle, The volume and composition of melt generated by extension of the lithosphere, J. Petrol. 29 (1988) 625–679.

[11] R.C.O. Gill, A.K. Pedersen, J.G. Larsen, Tertiary picrites in West Greenland: melting at the periphery of a plume? in: B.C. Storey, T. Alabaster, R.J. Pankhurst (Eds.), Magmatism and the Causes of Continental Break-up, Geol. Soc. London Spec. Publ. 68 (1992) 335–348.

[12] D.A. Clague, W.S. Weber, J.E. Dixon, Picritic glasses from Hawaii, Nature 353 (1991) 553–556.

[13] R.N. Thompson, S.A. Gibson, Extremely magnesian olivines in Phanerozoic picrites signify transient high temperatures during mantle plume impact, Nature 407 (2000) 502–506.

[14] E.J. Hanski, Petrology of the Pechenga ferropicrites and cogenetic, Ni-bearing gabbro wehrlite intrusions, Kola Peninsula, Russia, Geol. Surv. Finland Bull. 367, 1992, 192 pp.

[15] M. Fram, C.E. Lesher, Generation and polybaric differentiation of East Greenland Early Tertiary Flood Basalts, J. Petrol. 38 (1997) 231–275.

[16] P.C. Lightfoot, A.J. Naldrett, N.S. Gorbachev, W. Doherty, V.A. Federenko, Geochemistry of the Siberian Trap of the Noril'sk area, USSR, with implications for the relative contributions of crust and mantle to flood basalt magmatism, Contrib. Mineral. Petrol. 104 (1990) 631–644.

[17] J.L. Wooden, G.K. Czamanske, V.A. Federenko, N.T. Arndt, C. Chauvel, R.M. Bouse, B.W. King, R.J. Knight, D.F. Siems, Isotopic and trace-element constraints on mantle and crustal contributions to Siberian continental flood-basalts, Noril'sk area, Siberia, Geochim. Cosmochim. Acta 57 (1993) 3677–3704.

[18] K.G. Cox, C.J. Hawkesworth, Geochemical stratigraphy of the Deccan Traps at Mahabaleshwar, Western Ghats, India, with implications for open system magmatic processes, J. Petrol. 26 (1985) 355–377.

[19] J.E. Beane, P.R. Hooper, A note on the picritic basalts of the western Ghats, Deccan Traps, India, Geol. Soc. India Mem. 10 (1988) 117–133.

[20] B. Hanson, J.H. Jones, The systematics of Cr^{3+} and Cr^{2+} partitioning between olivine and liquid in the presence of spinel, Am. Mineral. 83 (1998) 669–684.

[21] S.R. Hart, K.E. Davis, Nickel partitioning between olivine and silicate melt, Earth Planet. Sci. Lett. 40 (1978) 203–219.
[22] R.O. Sack, M.S. Ghiorso, Chromian spinels as petrogenetic indicators: Thermodynamics and petrological applications, Am. Mineral. 76 (1991) 827–847.
[23] A. Kilinc, I.S.E. Carmichael, M.L. Rivers, R.O. Sack, The ferric–ferrous ratio of natural silicate liquids equilibrated in air, Contrib. Mineral. Petrol. 83 (1983) 136–140.
[24] J.R. Holloway, V. Pan, G. Gudmundsson, High pressure fluid-absent melting experiments in the presence of graphite: oxygen fugacity, ferric/ferrous ratio and disolved CO_2, Eur. J. Mineral. 4 (1992) 105–114.
[25] P. Ulmer, The dependence of the Fe^{2+}–Mg cation partitioning between olivine and basaltic liquid on pressure, temperature and composition, Contrib. Mineral. Petrol. 101 (1989) 261–273.
[26] D. Richard, B. Marty, M. Chaussidon, N.J. Arndt, Helium isotopic evidence for a lower mantle component in depleted Archean komatiite, Science 273 (1996) 93–95.
[27] C. Herzberg, Depth and degree of melting of komatiites, J. Geophys. Res. 97 (1992) 4521–4540.
[28] M.J. Walter, Melting of garnet peridotite and the origin of komatiite and depleted lithosphere, J. Petrol. 39 (1998) 29–60.
[29] J.C. Green, K.L. Schultz, Iron-rich basaltic komatiites in the early Precambrian Vermillion District, Minnesota, Can. J. Earth Sci. 14 (1977) 2181–2191.
[30] Q. Xie, R. Kerrich, J. Fan, HFSE/REE fractionations recorded in three komatiite-basalt sequences, Archean Abitibi greenstone belt; implications for multiple plume sources and depths, Geochim. Cosmochim. Acta 57 (1993) 4111–4118.
[31] K.Y. Tomlinson, D.J. Hughes, P.C. Thurston, R.P. Hall, Plume magmatism and crustal growth at 2.9 to 3.0 Ga in the Steep Rock and Lumby Lake area, western Superior Province, Lithos 46 (1999) 103–136.
[32] R. Kerrich, D. Wyman, P. Hollings, A. Polat, Variability of Nb/U and Th/La in 3.0 to 2.7 Ga Superior Province ocean plateau basalts; implications for the timing of continental growth and lithosphere recycling, Earth Planet. Sci. Lett. 168 (1999) 101–115.
[33] C. Herzberg, J. Zhang, Melting experiments on anhydrous peridotite KLB-1: composition of magmas in the upper mantle and transition zone, J. Geophys. Res. 101 (1996) 8271–8295.
[34] E.J. Hanski, V.F. Smolkin, Iron and LREE-enriched mantle source for early Proterozoic intraplate magmatism as exemplified by the Pechenga ferropicrites, Kola Peninsula, Russia, Lithos 34 (1995) 107–125.
[35] T. Kawamoto, J.R. Holloway, Melting temperature and partial melt chemistry of H_2O-saturated mantle peridotite to 11 gigapascals, Science 276 (1997) 240–243.
[36] W.E. Stone, E. Deloule, M.S. Larson, C.M. Lesher, Evidence for hydrous melts in the Precambrian, Geology 25 (1997) 143–146.
[37] E.H. Hauri, Major-element variability in the Hawaiian mantle plume, Nature 382 (1996) 415–419.
[38] R.D. Van der Hilst, S. Widiyantoro, E.R. Engdahl, Evidence for deep mantle circulation from global tomography, Nature 386 (1997) 578–584.
[39] M.J. Cordery, G.F. Davies, I.H. Campbell, Genesis of flood basalts from eclogite-bearing mantle plumes, J. Geophys. Res. 102 (1997) 20179–20197.
[40] E. Takahashi, K. Nakajima, D. Wright, Origin of the Columbia River basalts: Melting model of a heterogeneous plume head, Earth Planet. Sci. Lett. 162 (1998) 63–80.
[41] G.M. Yaxley, D.H. Green, Reactions between eclogite and peridotite: mantle refertilisation by subduction of oceanic crust, Schweiz. Mineral. Petrogr. Mitt. 78 (1998) 243–255.
[42] I. Kushiro, Partial melting of a fertile mantle peridotite at high pressures: An experimental study using aggregates of diamond, AGU Monogr. 95 (1996) 109–122.
[43] A. Yasuda, T. Fujii, K. Kurita, Melting phase relations of an anhydrous mid-ocean ridge basalt from 3 to 20 GPa: implications for the behaviour of subducted oceanic crust in the mantle, J. Geophys. Res. 99 (1994) 9401–9414.
[44] M.M. Hirschmann, Mantle solidus: Experimental constraints and the effects of peridotite composition, Geochem. Geophys. Geosyst. 1,
[45] G.M. Yaxley, Experimental study of the phase and melting relations of homogeneous basalt+peridotite mixtures and implications for the petrogenesis of flood basalts, Contrib. Mineral. Petrol. 139 (2000) 326–338.
[46] U.R. Christensen, A.W. Hofmann, Segregation of subducted oceanic crust in the convecting mantle, J. Geophys. Res. 99 (1994) 19867–19884.
[47] N.T. Arndt, A.J. Naldrett, D.R. Pyke, Komatiitic and iron-rich tholeiitic lavas of Munro Township, northeast Ontario, J. Petrol. 18 (1977) 319–369.
[48] N.T. Arndt, C.M. Lesher, Fractionation of REEs by olivine and the origin of Kambalda komatiites, Western Australia, Geochim. Cosmochim. Acta 56 (1992) 4191–4204.
[49] M.J. Bickle, J.L. Orpen, E.G. Nisbet, A. Martin, Structure and metamorphism of the Belingwe Greenstone Belt and adjacent granite–gneiss terrain: the tectonic evolution of an Archaean craton, in: M.J. Bickle, E.G. Nisbet (Eds.), The Geology of the Belingwe Greenstone Belt, Zimbabwe: A Study of the Evolution of Archaean Continental Crust, Balkema, Rotterdam, 1993, pp. 39–68.
[50] P. Hollings, D. Wyman, Trace element and Sm–Nd systematics of volcanic and intrusive rocks from the 3 Ga Lumby Lake greenstone belt, Superior Province; evidence for Archean plume–arc interaction, Lithos 46 (1999) 189–213.
[51] K.P. Jochum, N.T. Arndt, A.W. Hofmann, Nb–Th–La in komatiites and basalts; constraints on komatiite petrogenesis and mantle evolution, Earth Planet. Sci. Lett. 107 (1991) 272–289.

[52] A.C. Kerr, G.F. Marriner, N.T. Arndt, J. Tarney, The petrogenesis of Gorgona komatiites, picrites and basalts: new field, petrographic and geochemical constraints, Lithos 37 (1996) 245–260.
[53] A.C. Kerr, The geochemistry of the Mull–Morvern Tertiary lava succession, NW Scotland: an assessment of mantle sources during plume related volcanism, Chem. Geol. 122 (1995) 43–58.
[54] Y. Lahaye, N.T. Arndt, G. Byerly, C. Chauvel, S. Fourcade, G. Gruau, The influence of alteration on the trace-element and Nd isotopic compositions of komatiites, Chem. Geol. 126 (1995) 43–64.
[55] C. Lecuyer, G. Gruau, C.R. Anhaeusser, S. Forcade, The origin of fluids and the effects of metamorphism on the primary chemical compositions of Barberton komatiites: new evidence from geochemical (REE) and isotopic (Nd, O, H, $^{39}Ar/^{40}Ar$) data, Geochim. Cosmochim. Acta 58 (1994) 969–984.
[56] C.S. Perring, S.J. Barnes, R.E.T. Hill, Geochemistry of komatiites from Forrestania, Southern Cross Province, Western Australia: evidence for crustal contamination, Lithos 37 (1996) 181–197.
[57] A. Polat, R. Kerrich, D.A. Wyman, Geochemical diversity in oceanic komatiites and basalts from the late Archean Wawa greenstone belts, Superior Province, Canada: trace element and Nd isotope evidence for a heterogeneous mantle, Precambrian Res. 94 (1999) 139–173.
[58] V. Rajmani, K. Shivkumar, G.N. Hanson, S.B. Shirey, Geochemistry and petrogenesis of amphibolites, Kolar schist belt, South India: Evidence for komatiitic magma derived by low percentages of melting of the mantle, J. Petrol. 26 (1985) 92–123.
[59] L. Slater, Melt generation beneath Iceland, Unpublished Ph.D thesis, University of Cambridge, 204 pp, 1997.
[60] D. McKenzie, R.K. O'Nions, Partial melt distributions from inversion of rare earth element concentrations, J. Petrol. 32 (1991) 1021–1091.
[61] C.K. Brooks, T.F.D. Nielsen, The Phanerozoic development of the Kangerdlugssuaq area, East Greenland. Meddelelser om Gronland Geosci. 9 (1982) 30 pp.
[62] D.R. Lowe, G.R. Byerly, Geologic evolution of the Barberton Greenstone Belt, South Africa, Geol. Soc. Am. Spec. Pap. 329, 319 pp, 1999.
[63] S.C. Milner, A.R. Duncan, A.M. Whittingham, A. Ewart, Trans-Atlantic correlation of eruptive sequences and individual silicic volcanic units within the Paraná-Etendeka igneous province, J. Volcanol. Geotherm. Res. 69 (1995) 137–157.
[64] J.-P. Li, H. O'Neill, Subsolidus phase relations in the system $MgO–SiO_2–Cr–O$ in equilibrium with metallic Cr, and their significance for the petrochemistry of chromium, J. Petrol. 36 (1995) 107–132.
[65] R. Renner, Cooling and crystallisation of komatiite flows from Zimbabwe, Unpublished PhD thesis, University of Cambridge, Cambridge, 1989, 162 pp.
[66] S. Eggins, Origin and differentiation of picritic arc magmas, Ambae (Aoba), Vanuatu, Contrib. Mineral. Petrol. 114 (1993) 79–100.
[67] V.S. Kamenetsky, A.V. Sobolev, J.-L. Joron, M.P. Semet, Petrology and geochemistry of Cretaceous ultramafic volcanics from eastern Kamchatka, J. Petrol. 36 (1995) 637–662.
[68] M.B. Baker, S. Alves, E.M. Stolper, Petrography and petrology of the Hawaii Scientific Drilling Project: inferences from olivine phenocryst abundances and compositions, J. Geophys. Res. 101 (1996) 11715–11728.
[69] M.O. Garcia, Petrography and olivine and glasss chemistry of lavas from the Hawaii Scientific Drilling Project, J. Geophys. Res. 101 (1996) 11701–11715.
[70] L.A. Van Heerden, A.P. Le Roex, Petrogenesis of picrite and associated basalts from the southern mid-Atlantic ridge, Contrib. Mineral. Petrol. 100 (1988) 47–60.
[71] M.S. Ghiorso, I.S.E. Carmichael, Modeling magmatic systems: petrologic applications, Rev. Min. 17 (1988) 467–499.
[72] J. Myers, H.P. Eugster, The system Fe–Si–O: oxygen buffer calibrations to 1500 K, Contrib. Mineral. Petrol. 82 (1983) 75–90.
[73] P.A.H. Scowen, P.L. Roeder, R.T. Helz, Reequilibration of chromite within Kilauea lava lake, Hawaii, Contrib. Mineral. Petrol. 107 (1991) 8–20.
[74] W.E. Stone, J.H. Crockett, A.P. Dickin, M.E. Fleet, Origin of Archean ferropicrites: geochemical constraints from the Boston Creek flow, Abitibi greenstone belt, Ontario, Canada. Chem. Geol. (1995) 51–71.